Synthesis of Single-Crystalline TiO_2 Nanotubes

S. M. Liu,[†] L. M. Gan,[†] L. H. Liu,[‡] W. D. Zhang,[†] and H. C. Zeng*[,‡,§]

Institute of Materials Research and Engineering, 3 Research Ling, Singapore 117602, Department of Chemical and Environmental Engineering, Faculty of Engineering, and Chemical and Process Engineering Center, National University of Singapore, 10 Kent Ridge Crescent, Singapore 119260

Received October 15, 2001. Revised Manuscript Received January 2, 2002

In this work, we demonstrate experimentally that the classification of "inorganic fullerene-like structures" can be extended from transition metal sulfides to include metal oxides. Single-crystalline TiO_2 nanotubes have been synthesized for the first time with an unconstrained solution growth method by hydrolyzing TiF_4 under acidic condition at 60 °C. With SEM/HRTEM/XRD methods, it is found that the walls of TiO_2 tubes are formed with stacking of {101} planes (anatase polymorph). Both HRTEM and XRD indicate an interplanar spacing of $d_{101} = 0.36 \pm 0.01$ nm in the wall structure. Although the {101} planes can be curved into concentric cylinders, straight segments of {101} planes are also observed. The inner diameters of the tubes are in the range of 2.5−5 nm, and outer diameters are in the range of 20−40 nm with lengths up to a few hundred nanometers. Similar to the well-known fullerene-like nanotubes formed from layered materials (graphite, MoS_2, and WS_2), spherical and polyhedral closings for the TiO_2 nanotubes are observed. Anodic aluminum oxide nanochannels and alumina nanoparticles have been used to differentiate growth modes and to address the role of solid substances in TiF_4 hydrolysis. It is revealed that TiO_2 can still be synthesized in the form of fullerene-like inorganic nanotubes, although it is not a layered compound. Future directions in this research area are also discussed.

Introduction

In recent years, research in nanotube materials has been developed into many new areas since Iijima's discovery of carbon nanotubes (CNTs) in 1991.[1−5] In particular, inorganic nanotubes such as fullerene-like nanotubes (e.g., MS_2, M = Mo, W, Nb, Ta, etc.) have been synthesized.[6−9] It is noted that the metal dichalcogenides have layered structures analogical to the fullerene materials (e.g., CNTs), and the layers are held together mainly by weak van der Waals forces. This, in turn, lowers the rigidity of the planes in turning into tubular morphology.[2,3,6]

Unlike the above layered compounds, many important metal oxides such as TiO_2, ZnO, MnO_2, ZrO_2, Co_3O_4, etc are not layered materials, and the strong ionic interactions hold together the metal cations and oxygen anions that normally show a strong tendency in crystallization at elevated temperatures during the lattice formation. Despite of the great difficulties, research in tube formation for this class of materials has been significantly advanced.[10−22] The important progress includes synthesis of transition metal oxide nanotubes (e.g., TiO_2) from anodic aluminum oxide templates (AAO, including replicated PMMA negatype from AAO) and supramolecular templates with various sol−gel methods that transfer materials onto inner or outer surfaces of templates.[10−16]

Because the metal oxide nanotubes are converted from the amorphous gels supported on solid templates

* To whom correspondence should be addressed. E-mail: chezhc@nus.edu.sg.
[†] Institute of Materials Research and Engineering.
[‡] Department of Chemical and Environmental Engineering, National University of Singapore.
[§] Chemical and Process Engineering Center, National University of Singapore.

(1) Iijima, S. *Nature* **1991**, *354*, 56.
(2) Ajayan, P. M.; Ebbesen; T. W. *Rep. Prog. Phys.* **1997**, *60*, 1025.
(3) Subramoney, S. *Adv. Mater.* **1998**, *10*, 1157.
(4) Ebbesen, T. W.; Ajayan, P. M. *Nature* **1992**, *358*, 220.
(5) Thess, A.; Lee, R.; Nikolaev, P.; Dai, H.; Petit, P.; Robert, J.; Xu, C.; Lee, Y. H.; Kim, S. G.; Rinzler, A. G.; Colbert, D. T.; Scuseria, G. E.; Tomanek, D.; Fischer, J. E.; Smalley, R. E. *Science* **1996**, *273*, 483.
(6) Tenne, R.; Homyonfer, M.; Feldman, Y. *Chem. Mater.* **1998**, *10*, 3225 and references therein.
(7) Feldman, Y.; Frey, G. L.; Homyonfer, M.; Lyakhovitskaya, V.; Margulis, L.; Cohen, H.; Hodes, G.; Hutchison, J. L.; Tenne, R. *J. Am. Chem. Soc.* **1996**, *118*, 5362.
(8) Zak, A.; Feldman, Y.; Alperovich, V.; Rosentsveig, R.; Tenne, R. *J. Am. Chem. Soc.* **2000**, *122*, 11108.
(9) Nath, M.; Rao, C. N. R. *J. Am. Chem. Soc.* **2001**, *123*, 4841.
(10) Lakshmi, B. B.; Patrissi, C. J.; Martin, C. R. *Chem. Mater.* **1997**, *9*, 2544 and references therein.
(11) Zhang, M.; Bando, Y.; Wada, K. *J. Mater. Sci. Lett.* **2001**, *20*, 167.
(12) Zhang, M.; Bando, Y.; Wada, K. *J. Mater. Res.* **2001**, *16*, 1408.
(13) Kobayashi, S.; Hanabusa, K.; Hamasaki, N.; Kimura, M.; Shirai, H. *Chem. Mater.* **2000**, *12*, 1523.
(14) Hippe, C.; Wark, M.; Lork, E.; Schulz-Ekloff, G. *Microporous Mesoporous Mater.* **1999**, *31*, 235.
(15) Hoyer, P. *Langmuir* **1996**, *12*, 1411.
(16) Hoyer, P. *Adv. Mater.* **1996**, *8*, 857.
(17) Lencka, M. M.; Riman, R. E. *Chem. Mater.* **1993**, *5*, 61.
(18) Imai, H.; Takei, Y.; Shimizu, K.; Matsuda, M.; Hirashima, H. *J. Mater. Chem.* **1999**, *9*, 2971.
(19) Shimizu, K.; Imai, H.; Hirashima, H.; Tsukuma, K. *Thin Solid Films* **1999**, *351*, 220.
(20) Imai, H.; Matsuda, M.; Shimizu, K.; Hirashima, H.; Negishi, N. *J. Mater. Chem.* **2000**, *10*, 2005.
(21) Kasuga, T.; Hiramatsu, M.; Hoson, A.; Sekino, T.; Niihara, K. *Langmuir* **1998**, *14*, 3160.
(22) Kasuga, T.; Hiramatsu, M.; Hoson, A.; Sekino, T.; Niihara, K. *Adv. Mater.* **1999**, *11*, 1307.

10.1021/cm0115057 CCC: $22.00 © 2002 American Chemical Society
Published on Web 02/16/2002

after thermal treatments, polycrystalline walls are commonly obtained, although the crystallization temperatures for these sol−gel derived materials have been lowered. Recent efforts have been directed to low-temperature routes using some known chemical reactions of TiO_2 precursors.[17−22] For example, polycrystalline TiO_2 nanotubes have been prepared using the hydrolysis reactions of TiF_4 in the AAO templates at pH = 2.0 and 40−70 °C.[18−20] Furthermore, it has been reported that TiO_2 nanotubes can be prepared in aqueous phase with various base−acid treatments at 110 °C from the same raw materials, although single crystallinity of the nanotubes has not been confirmed so far.[21,22]

Among the oxide nanotubes, TiO_2 is one of the most investigated oxide materials owing to its technological importance. It has been widely used for photocatalysis and environmental cleanup applications, due to its strong oxidizing power, chemical inertness, and nontoxicity.[17−22] For example, polycrystalline TiO_2 nanotubes have many important applications such as separations and analytical sensing due to presence of interparticle pores within the tube walls in addition to the tube cavities.[10,18] To fully utilize these 1D materials, it would also be highly desirable to prepare single-crystalline TiO_2 nanotubes to take advantage of their anisotropic properties in many low-dimensional electronic applications.[23] In this article, as a part of our recent efforts in "soft" chemical synthesis of nanotube materials,[24] we report the first synthesis of single-crystalline TiO_2 nanotubes using an unconstrained growth method in aqueous solution at only 60 °C without any post-growth thermal treatments. Quite surprisingly, nonlayered ionic compound TiO_2 can be prepared in the form of "inorganic fullerene-like nanotubes".[1−9]

Experimental Section

The AAO membranes were prepared by a two-step anodization process with the treatments described in the literature.[25] Anodic oxidation of aluminum (10 × 50 × 0.5 mm) was conducted under a constant voltage of 40 V for 10 h in a solution of oxalic acid (0.30 M). The anodic oxide film was chemically removed using a solution of phosphoric and chromic acid (20 g pure chromic acid powder and 35 cm^3 phosphoric acid (85.6 wt %) mixed with deionized water to 1.0 L) which did not attack aluminum but dissolved the thin oxide film. After removal of the anodic layer, the textured aluminum sheet was anodized again for 20−40 h under the same conditions as described in the first anodization. After coating a protective layer on the surface of the porous AAO membrane, the remaining Al layer was dissolved by placing the protected anodized sheet in a solution of HCl (32%) and $CuCl_2$ (0.05%). A subsequent etching treatment was carried out in a 5 wt % phosphoric acid solution at room temperature for 3 h to remove the barrier layer on the bottom side of the AAO membrane. After the protective layer was dissolved in acetone, a uniform through-hole AAO membrane was obtained.

Hydrochloric acid (HCl) and aqueous ammonia (NH_4OH) were used to adjust pH of deionized water (1.0 L) to 2.1. Titanium tetrafluoride (TiF_4, Aldrich Chemical) was then dissolved in this solution to give a concentration of 0.04 M, during which pH was changed to 1.6. The required amount (100 mL) of TiF_4 solution and the AAO membranes were transferred to a closed glass flask, which was maintained at 60 °C for a certain period of time (12, 24, and 48 h). To investigate the possible formation routes of TiO_2 nanotubes, the AAO membranes were replaced by Al_2O_3 nanoparticles in the synthesis (48 h). For a better comparison, pure TiO_2 nanotube samples were prepared only with TiF_4 solution (i.e., without adding the AAO templates or Al_2O_3 nanoparticles) with different processing times (7, 23, 48, and 63 h). The products were washed with deionized water and dried at 60 °C for 24 h.

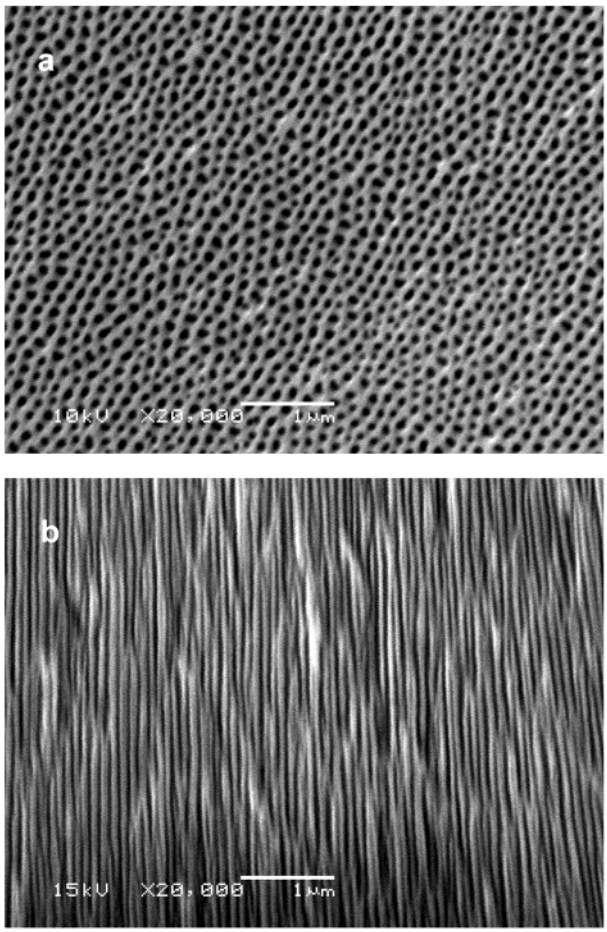

Figure 1. SEM images of the homemade AAO membrane with an averaged hole diameter of 100 nm and membrane thickness of 60 μm: (a) surface view and (b) cross-sectional view; the sample was prepared in 0.30 M oxalic acid solution (1st anodization, 10 h and 2nd anodization, 20 h).

Crystalline phase of TiO_2 was determined by X-ray diffraction method (XRD, Shimadzu XRD-6000, Cu Kα radiation). Structures of the prepared AAO membranes and TiO_2 nanotubes were examined using scanning electron microscope (SEM, Hitachi Model S-4100) and high-resolution transmission electron microscope (HRTEM, Philips FEG CM300; at 300 kV). Chemical compositions of the crystallized TiO_2 products after hydrolysis reactions were investigated with energy dispersive spectroscopy (EDX, JSM-5600LV). The specimen for HRTEM imaging was prepared by suspending 2 mg of the powder sample with acetone and sonicating in an ultrasonic bath for 30 min.[24]

Results and Discussion

Figure 1 shows two SEM images of the as-prepared porous AAO templates after 10 + 20 h anodization in 0.30 M oxalic acid solution. The pores are evenly distributed on the surface with a distorted hexagonal pattern; it was noted that most of the pores have six

(23) Cassagneau, T.; Fendler, J. H.; Johnson, S. A.; Mallouk, T. E. *Adv. Mater.* **2000**, *12*, 1363.
(24) (a) Ji, L.; Lin, J.; Zeng, H. C. *Chem. Mater.* **2000**, *12*, 3466. (b) Xu, Z. P.; Zeng, H. C. *J. Phys. Chem. B* **2000**, *104*, 10206. (c) Xu, Z. P.; Xu, R.; Zeng, H. C. *Nano Lett.* **2001**, *1*, 703.
(25) Masuda, H.; Tanaka, H.; Baba, N. *Chem. Lett.* **1990**, 621.

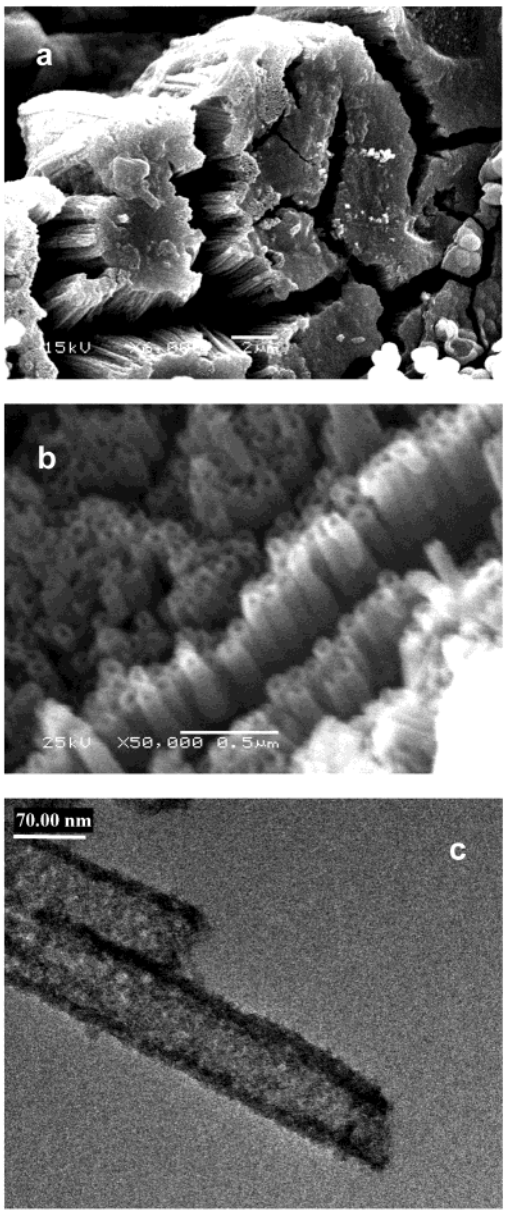

Figure 2. Polycrystalline anatase TiO_2 nanotubes synthesized with AAO template (of Figure 1) for 12 h: (a) SEM image of TiO_2 bundles, (b) SEM image of unidirectionally aligned TiO_2 nanotubes, and (c) TEM image of two TiO_2 nanotubes formed with nanocrystalline TiO_2 particles.

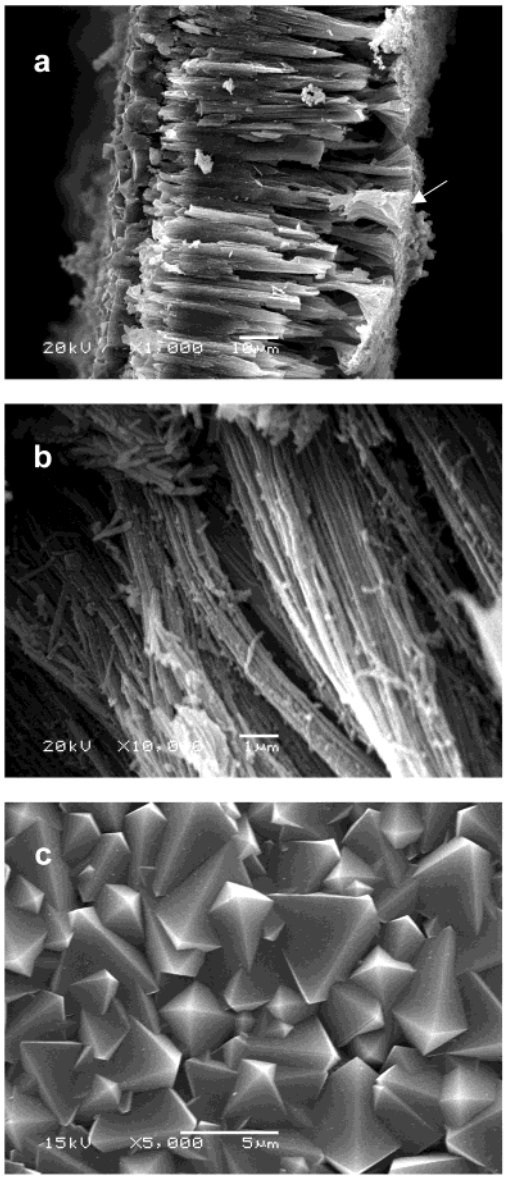

Figure 3. SEM images of polycrystalline nanotubes and crystallites/crystals of anatase TiO_2 synthesized with AAO template (of Figure 1) for 12 h: (a) overall morphology (TiO_2 + AAO membrane (some of which has been peeled off)), (b) detailed view of TiO_2 nanotubes in the middle section of (a), and (c) single crystals of TiO_2 formed on the bottom surface of the AAO membrane; broccoli-like crystallites formed on the top are indicated by an arrow.

neighbors while some have five or seven. A cross-sectional examination indicated that these one-dimensional pores (1D channels) indeed extend vertically into the AAO membrane. The averaged channel size is ca. 100 nm in diameter and 60 μm in length, with a density of 4×10^9 cm^{-3}. With the use of these homemade AAO templates, the direct synthesis of TiO_2 nanotubes in the 1D channels was carried out by hydrolyzing TiF_4 solution (pH = 1.6), as described in Experimental Section. Some representative SEM/TEM images of the TiO_2 nanotubes are displayed in Figure 2. Similar to the reported literature, the formed nanotubes are in bundle form perpendicular to the surface of the AAO membrane (Figure 2a).[18] Although they were prepared directly at low temperature (Figure 2b), the TiO_2 nanotubes have a similar tubule structure as that derived from a sol−gel route (calcined at 400 °C in air).[10] The walls of the tubes, however, comprise small crystallites of TiO_2 as detailed in the TEM image (Figure 2c). Similar observation of this type of nanotubes has been reported using the SEM method, and the formation of polycrystalline nanotubes has been attributed to the heterogeneous nucleation on the inner walls of the 1D channels.[18] Indeed, this postulation is further supported by our observation that the averaged outer tube diameter is identical to the averaged channel diameter. As the surface of AAO channels serves as a template, multiple nucleations are expected to take place simultaneously all over the places of inner walls, resulting in the polycrystalline nanotubes.

In addition to the above known observations for the confined nanotubes, it is surprising to find that the top of AAO membrane is covered with broccoli-like fine crystallites of TiO_2 whereas much larger crystals were

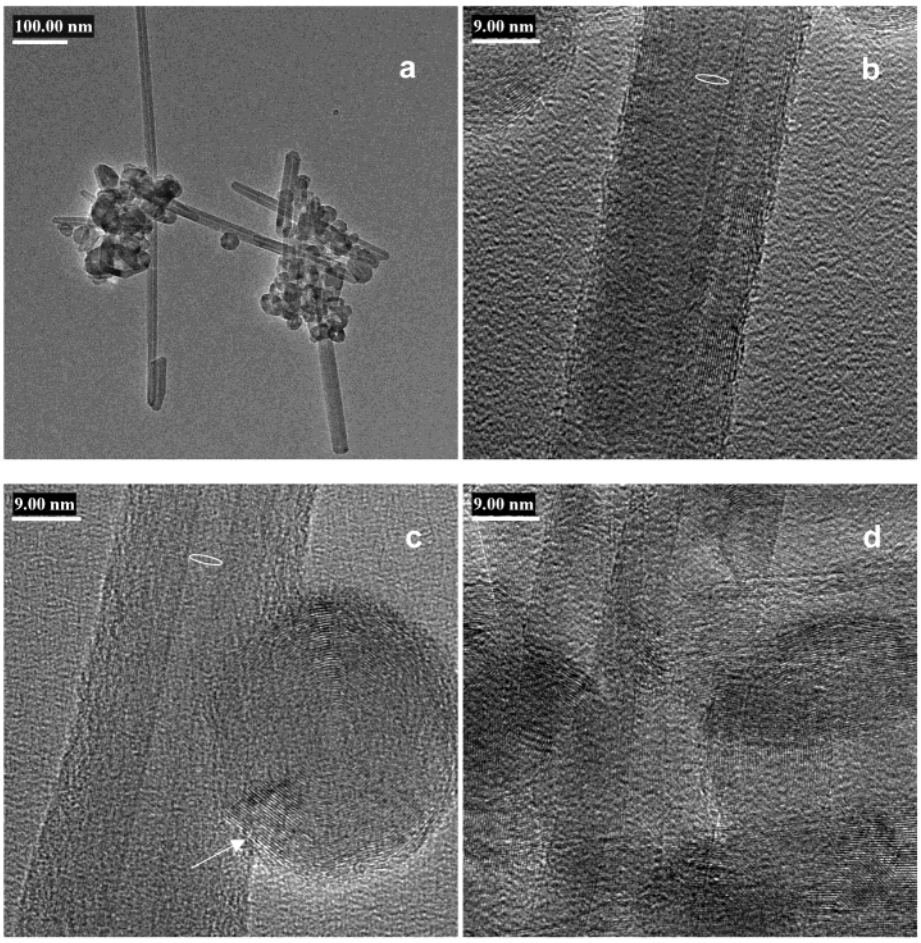

Figure 4. HRTEM images of single-crystalline anatase TiO_2 nanotubes with a synthesis time of 12 h (formed together with those in Figure 3): (a) overall view, (b) detailed view on the tube structure, (c) an onion-like structure attaching to a tube, and (d) detailed view on an assembly part in (a).

formed on the bottom surface of AAO membrane. Shown in Figure 3 are some SEM micrographs taken from different portions of a reacted AAO membrane. Similar to the case of polycrystalline TiO_2 nanotubes, the AAO membrane surface may provide nucleation sites for the crystallite growth. Furthermore, the grown polycrystalline TiO_2 nanotubes at the channel openings may act as seeds for the extended growth (Figure 3a). It should be pointed out that this cover prevents the nanotubes that are underneath from growing into solid rods. On the other hand, TiO_2 crystals formed on the bottom surface of AAO membrane are single crystals in tetragonal symmetry (anatase phase; XRD method);[26] it is noted that the {101} facets and both C_2 and C_4 rotation symmetries can be clearly observed (Figure 3c).[27] The size of these crystals is about 2−5 μm, which is much larger than the broccoli-like crystallites, and they show a compact crystal assembly with random orientations. Therefore, the crystal morphology may reflect a low supersaturation growth (note that this surface was in contact with the bottom of the glass flask: smaller volume of liquid and thus less nutrient was available). With prolonged processing times (24 and 48 h), the crystallites/crystals on the AAO membrane surfaces grew into thicker layers, while more and more crystallite nuclei were deposited on the external surfaces of polycrystalline TiO_2 nanotubes that were separated from channel templates. These findings seem to suggest that there is a possibility of growing other single-crystalline nanostructures of TiO_2 using the hydrolysis of TiF_4 in aqueous solution. Indeed, single-crystalline TiO_2 nanotubes are present in our samples, which is the main concern of this paper.

As shown in Figure 4, the single-crystalline TiO_2 are normally aggregated (Figure 4a), although individual nanotubes or onions can be separated with extended sonicating. The tubules are very straight with clear cavities in the axial direction. The outer diameters are about 20−40 nm while the inner diameters (marked with white rings) are around 4−5 nm for most of the nanotubes. Various aspect ratios (the length of the tubes can be as long as a few hundred nanometers) and the excellent crystallinity are noted. The single crystallinity of these nanotubes is unambiguously evidenced by the highly resolved TiO_2 lattice fringe details (see HRTEM images in Figures 4 to 7),[28] while their crystal structure is confirmed with XRD method. The nearest layers in the tube walls are strictly separated in all cases by a plane distance of 0.36 ± 0.01 nm, which corresponds to

(26) Joint Committee on Powder Diffraction Standards, International Centre for Diffraction Data, Swarthmore, PA, 1996: Anatase TiO_2 (#21−1272).

(27) (a) Zeng, H. C.; Chong, T. C.; Lim, L. C.; Kumagai, H.; Hirano, M. *J. Cryst. Growth* **1994**, *140*, 148. (b) Zeng, H. C.; Lim, L. C. *J. Mater. Res.* **1998**, *13*, 1426.

(28) Penn, R. L.; Banfield, J. F. *Science* **1998**, *281*, 969.

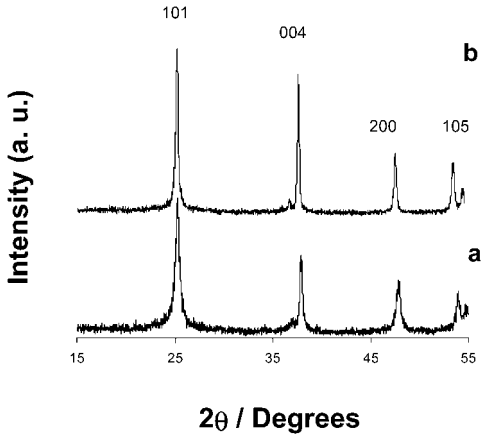

Figure 5. XRD patterns for (a) mixed samples of the reacted AAO membranes that include mainly polycrystalline TiO_2 nanotubes (i.e., solid AAO samples from three experiments of 12, 24, and 48 h) and (b) pure single-crystalline anatase TiO_2 nanotubes and nanoparticles (unconstrained synthesis, 48 h, Figure 6d).

the interplanar spacing of d_{101} in the anatase polymorph.[26,28] When related to the crystal morphologies of Figure 3, it is not difficult to understand why the TiO_2 nanotubes adopt the natural planes of {101} as their wall surfaces. The constant inner diameter of ca. 4−5 nm (Figures 4a and 4b) may reflect a tolerable curvature that {101} planes can sustain in forming interior walls. Although the inner surfaces are flat and smooth, outer surfaces of the tubes are generally rougher. This indicates that while a tube grows along its axial direction, external surface growth occurs simultaneously. Since the latter growth can take place on an entire surface, outer surfaces of the tubes are rougher. According to the growth time, furthermore, the outer diameters of the tubes can be varied (Figure 4c). Nonetheless, the axial growth is still a predominant growth mode, compared to the external surface deposition. It is expected that in rolling a flat plane of {101} into a cylindrical tubule, strains must be present in the walls. Indeed, our HRTEM examination on both the tubes and onions shows that straight segments (marked with an arrow) exist although an overall concentric shape can still be achieved via connecting both curved and straight segments together (Figures 4a and 4c), which will be further elucidated shortly. This finding, on the other hand, confirms the presence of TiO_2 structure, as the nanotubes are constructed from the original flat TiO_2. In excellent agreement with these observations, the XRD pattern recorded in Figure 5 for the above samples shows that the (101) reflection ($d_{101} = 0.353 \pm 0.001$ nm) is the strongest among the anatase peaks while the AAO templates are largely in an amorphous state (Figure 4a).[26]

Since the outer diameters of the above nanotubes are much smaller than that of the AAO channels, the template growth can be ruled out unambiguously. Furthermore, the observed high crystallinity seems to suggest that the TiO_2 nanotubes were grown in an

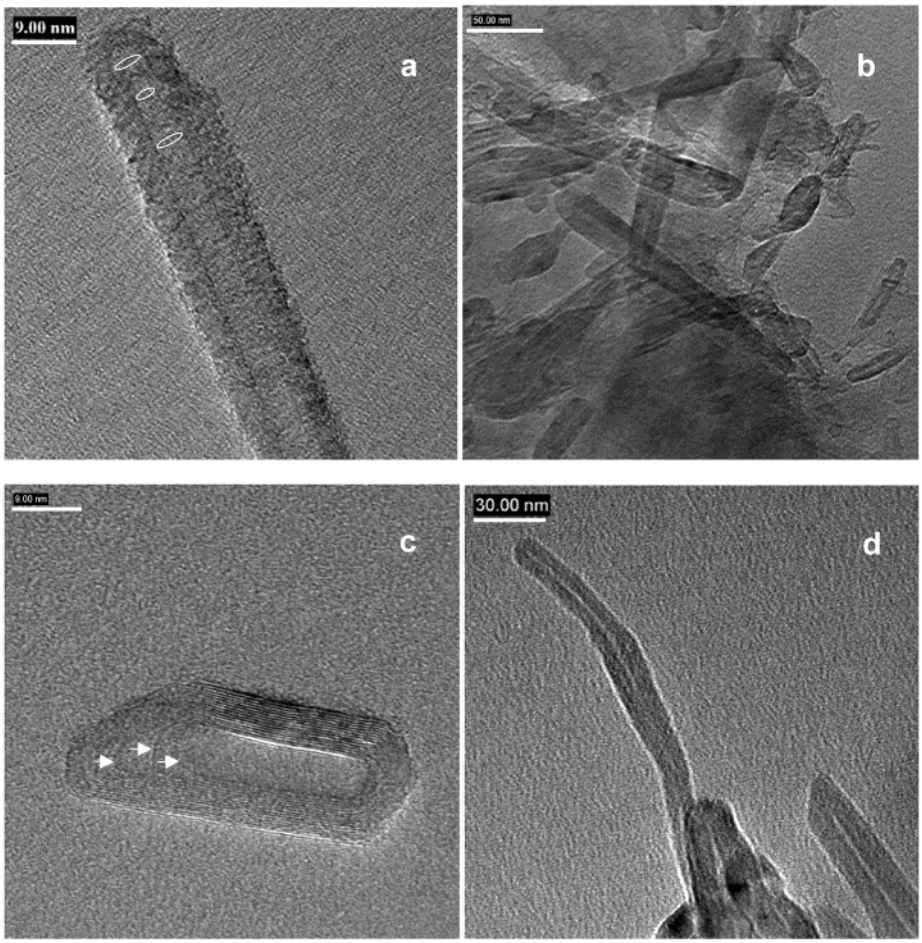

Figure 6. HRTEM images of single-crystalline anatase TiO_2 nanotubes prepared with Al_2O_3 nanoparticles for a synthesis time of 48 h (a) and prepared without adding any solid substances (unconstrained synthesis) for 7 h (b), 23 h (c), and 48 h (d), respectively.

unconstrained manner; it is noted that the AAO membrane surface or the formed polycrystalline TiO_2 nanotubes could act as nucleation sites/seeds for this secondary growth. To verify this assumption, nanoparticles of Al_2O_3 were added to the solution in replacement of the AAO membranes. Similar to those shown in Figure 4, highly crystalline TiO_2 nanotubes were also produced. As an example, shown in Figure 6a, the nanotube wall comprises only 10−11 layers with a bamboo type of closing. The inner diameter of the tube is reduced from ca. 4 nm to 2.5 nm and then returned to 4 nm at the top portion (marked with white rings). Similar to those in the growth of CNTs in vapor phase,[29,30] the bamboo-like endings indicate that the inner layers make a turn first while the outer layers grow continuously during the capping process. Because there is no direct correlation between the size of Al_2O_3 powder (10 nm) and the observed inner and outer diameters, it is thought that the Al_2O_3 nanoparticles do not act as a template either. Nevertheless, the catalytic effect of Al_2O_3 on the TiF_4 hydrolysis cannot be excluded at this stage. Without adding the Al_2O_3 nanoparticles, in a further test for the above point, we found that similar single-crystalline TiO_2 nanotubes could also be prepared (Figures 6b−6d). The bamboo-like closure in Figure 6c shows that even single or double layers of {101} planes can be stabilized in the TiO_2 nanotubes, which is an analogue to single-walled carbon nanotubes.[1−5] Furthermore, in Figures 6c and 6d, both the spherical ending and the polyhedral ending can be clearly observed. To further confirm tubular structure, Figure 7 shows a pair of HRTEM images taken along axial direction with focuses at two different levels. Although they are not perfectly round, the "fullerene-like sheets" are definitely continued to generate distorted concentric rings. The findings in all these experiments indicate that single-crystalline tubes were actually grown in an unconstrained manner, although solid substances (such as surfaces of AAO and Al_2O_3 or even SiO_2) might provide initial nucleation sites as in any common solution crystal growths.[31] In this agreement, it was observed that the white precipitates of TiO_2 nanotubes were indeed deposited on the surface of the reaction flask (made of glass). Powder XRD investigation (Figure 5, part b) of the white precipitates prepared without adding AAO or Al_2O_3 powder reveals that they indeed have a wall structure formed by {101} planes. In particular, the intense peak of (101) reflection ($d_{101} = 0.353 \pm 0.001$ nm) is now much narrower (Figure 5, part b vs part a), which indicates an increase in single crystallinity for the nanotubes in the unconstrained growth. Furthermore, the presence of fluorine and hydroxyl groups can be excluded. Chemical composition analyses reported in Table 1 indicate that the crystallized products after washing with deionized water are indeed at a strict stoichiometry of TiO_2.

The chemical reactions of TiF_4 hydrolysis in the formation of TiO_2 have been understood, which take place as in the following steps[17,19]

$$TiF_4 \rightarrow Ti(OH)_{4-x}F_x \rightarrow TiO_2 \qquad (1)$$

The single-crystalline tubes observed in the current work can be attributed to the low supersaturation in the growth. The low pH (1.6) ensures a slow hydrolysis of TiF_4 and thus a smooth growth of TiO_2 nanotubes. It is interesting to ask the question why TiO_2 adopts a tubular morphology rather than that of a 3D crystallite that seems to be thermodynamically more stable. To address this question, it is important to realize that the {101} crystallographic planes are the compact ones whereas the growths perpendicular to these planes are the slowest as evidenced in the facets formed in Figure

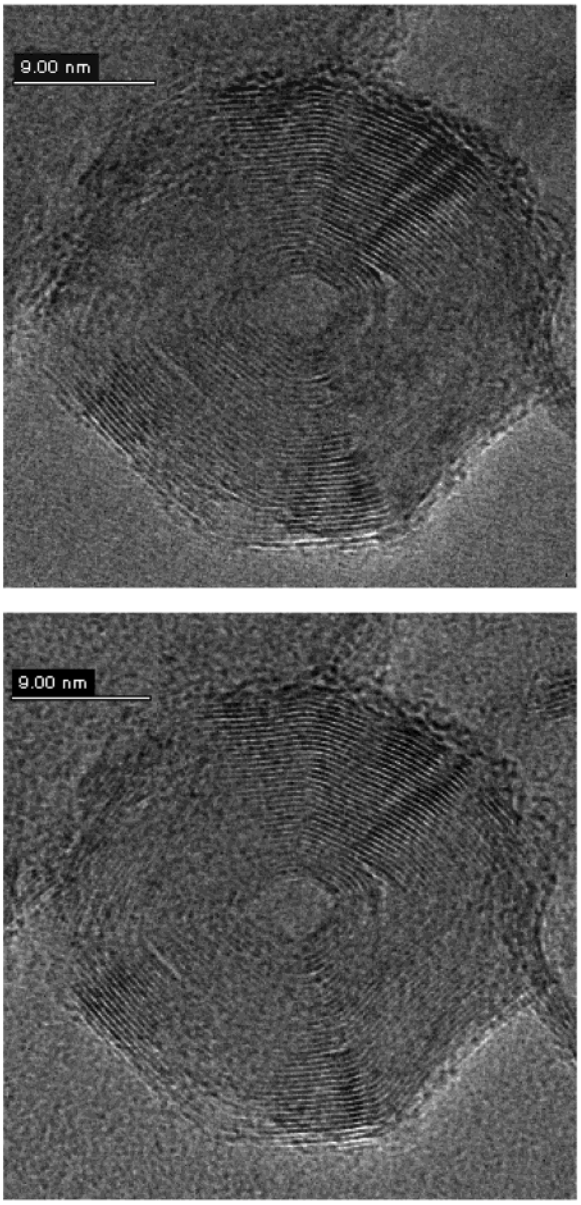

Figure 7. HRTEM images of a short single-crystalline anatase TiO_2 nanotube (unconstrained synthesis for 23 h) with different focuses along axial direction; continuous and concentric curving of {101} planes is clearly seen although some segments of the rings are flattened.

Table 1. EDX Elemental Analysis of Crystallized TiO_2

element	Ti (K)	O (K)	Pt (M)[a]	V (K)[b]	O/Ti
		Sample 1			
atomic %	29.93	69.09	0.98	0.00	
atomic ratio					2.31
		Sample 2			
atomic %	33.73	64.67	1.09	0.52	
atomic ratio					1.91
avg atomic ratio					2.11

[a] Due to Pt coating prior to the EDX measurement. [b] Impurity from the starting chemicals.

3. It is our belief that the attachment of hydrolyzing species (e.g., $Ti(OH)_{4-x}F_x$, eq 1) during the lateral growth of {101} planes may self-impose extra steric effects on the growing interfaces (i.e., the adsorbed species can access the growing interfaces only from certain angles), resulting in a curving tendency of the {101} planes to fold into the tubular structure. Further investigations using more bulky precursor compounds for hydrolysis should allow us to address this type of a question in detail.

In comparison to carbon nanotubes in which graphene layers are more flexible, the {101} sheets in the above TiO_2 nanotubes are much more rigid because of ionic interactions among these planes. The straight segments observed along the axial direction reflect the persistence of flat {101} planes in making these nanotubes. The tube structure of TiO_2, which depends on the intraplanar and interplanar distortions of Ti−O−Ti connectivity, may be stabilized by the large organic molecules/ions in synthetic solutions. Future investigations using micelles and supramolecular templates may help us to improve the symmetry, regularity, and morphological control of single-crystalline TiO_2 nanotubes, including the making of inorganic−organic nanohybrids.

Conclusions

In summary, single-crystalline TiO_2 nanotubes with lengths up to a few hundred nanometers can be synthesized using a simple solution route via the hydrolysis of TiF_4 at low pH with gentle heating at 60 °C. By the utilization of AAO templates and Al_2O_3 nanoparticles, it is confirmed that the single-crystalline TiO_2 nanotubes are prepared without the assistance of the solid templates, while the solid substances can provide initial nucleation sites for the unconstrained growth. Single-crystalline TiO_2 nanotubes are constructed with stacking of the {101} crystallographic planes of anatase phase, and the interplanar distance determined by HRTEM/XRD methods is consistently at $d_{101} = 0.36 \pm 0.01$ nm. Although an overall concentric stacking of the {101} planes is maintained in the tube structure, the flattened segments of {101} planes can still be seen in the walls, reflecting the persistence of the original anatase structure in turning into curved sheets. Due to this, polyhedral closing and fullerene-like capping are both observed in the nanotubes. In particular, analogical to the single-walled fullerene nanotubes, single or double-sheets of {101} can be stabilized during the tube closure process, as resolved in our HRTEM observations. The diameters of the inner tubes are in the range of 2.5−5 nm, and the diameters of the outer tubes are in the range of 20−40 nm. Although it does not have a layered structure, TiO_2 can actually utilize its {101} planes to build the highly crystalline nanotubes. It is recognized that interplanar interactions in the formed TiO_2 nanotubes are still largely ionic unlike the van der Waals interactions in carbon and metal dichalcogenide nanotubes. Future investigations using more bulky precursor compounds and/or introducing supramolecular templates in the synthesis may help one to improve tube symmetry and regularity.

Acknowledgment. The authors gratefully acknowledge research funding (RP3999902/A and A/C50384) cosupported by the Ministry of Education and the National Science and Technology Board of Singapore.

CM0115057

(29) Saito, Y. In *Carbon Nanotubes*; Endo, M., Iijima, S., Dresselhaus, M. S., Eds.; Pergamon: Oxford, 1996; p 153.
(30) Ugarte, D. In *Carbon Nanotubes*; Endo, M., Iijima, S., Dresselhaus, M. S., Eds.; Pergamon: Oxford, 1996; p 163.
(31) Brice, J. C. *Crystal Growth Processes*; John Wiley & Sons: New York, 1986; p 167.